Comparison of Torsional and Cyclic Fatigue Resistance of Various Nickel-titanium Single-file Systems

Gyeongha Son

The Graduate School

Yonsei University

Department of Dentistry

Comparison of Torsional and Cyclic Fatigue Resistance of Various Nickel-titanium Single-file Systems

A Master's Thesis
Submitted to the Department of Dentistry
And the Graduate School of Yonsei University
In partial fulfillment of the
Requirements for the degree of
Master of Dental Science

Gyeongha Son

June 2020

This certifies that the Master's Thesis of Gyeongha Son is approved.

김 선 일

Sunil Kim

Euiseong Kim

김 도 현

Dohyun Kim

The Graduate School

Yonsei University

June 2020

감사의 글

보존과 수련을 시작하며 모든 것이 부족하던 제가 임상 뿐만 아니라 연구를 함께 하는 시간들은 시작부터 막연하고도 어려운 시기였습니다. 하지만 이러한 저에게 소중한 가르침과 많은 도움을 주신 교수님들, 동기들, 선후배님들이 계셨기에 무사히 학위과정을 마무리 할 수 있었습니다. 바쁘신 와중에도 이번 연구와 학위 논문 작성 과정에서 많은 조언과 도움을 주시고, 아낌없이 지원을 해주신 김선일 지도교수님과 김의성 교수님께 진심으로 감사드립니다. 그리고 부족했던 제가 훌륭한 보존과 의사로 거듭날 수 있게 이끌어 주신 노병덕 교수님, 박성호 교수님, 정일영 교수님, 박정원 교수님, 신수정 교수님, 신유석 교수님, 김도현 교수님, 강수미 교수님께 깊이 감사드립니다.

보존과 수련 생활을 하면서 여러 힘든 순간들이 있었습니다. 하지만 그럴 때마다 격려해주고 기운을 북돋아 주었던 의국원들이 있었기에 힘을 내어 이 순간까지 올 수 있었습니다. 특히나 같은 시기를 보내며 서로에게 의지가 되었던 의국 동기들에게 큰 고마움을 느낍니다. 반면 저는 바쁘다는 핑계로 의국원들을 잘 챙겨주지 못한 것 같아 미안함이 많이 남습니다. 앞으로 남은 수련 기간동안 제가 받았던 것만큼 교수님들과 의국원들에게 보답하며, 마지막까지 흐트러지지 않는 모습을 보여드리기 위해 노력하겠습니다.

마지막으로 6 년의 치과대학 과정과 4 년의 전공의 과정이라는 긴 기간동안 많은 응원과 지원을 해주신 아버지, 어머니께 사랑과 감사의 마음을 전합니다.

2020 년 6 월

손 경 하

Table of Contents

List of Figures

List of Tables

Abstract

Comparison of Torsional and Cyclic Fatigue Resistance of Various Nickel-titanium Single-file Systems

Gyeongha Son, D.D.S.

Department of Dentistry

The Graduate School, Yonsei University

(Directed by Professor Sunil Kim, D.D.S., M.S.D., Ph.D.)

The aim of this study was to investigate and compare the torsional and cyclic fatigue resistance among three different-sized Ni-Ti files of each single-file system and among same-sized Ni-Ti files of three different single-file systems and to evaluate topographic of the fractured surface of instrument using scanning electron microscope and identify the characteristics of each fracture mechanism. Also, to investigate the martensite/austenite transformation temperatures of the three systems using differential scanning calorimetry analysis.

Three different single-file systems (Waveone Gold[WO]; Dentsply Sirona, Ballaigues, Switzerland, M3-L platinum[M3L]; United Dental Changzhou, Shanghai, China and Trunatomy[TN]; Dentsply Sirona) and three different sizes (#20, #25, #35) of each system were selected and ten brand new instruments of each file were evaluated per test. To evaluate the torsional resistance, 5 mm apical part of the instrument was rigidly fixed between 2 polycarbonate blocks and instruments were rotated continuously at speed of 2 rpm until fracture occurred. The ultimate load (Ncm), distortion angle at the fractured point (°), and the toughness (Ncm°) were measured. To evaluate the cyclic fatigue resistance, the number of cycles to fracture (NCF) for each instrument was measured in artificial canal block. After the tests, fractured surfaces of instruments representing each group were evaluated using scanning electron microscope to evaluate topographic of the fractured surface. And to investigate the phase transformation temperatures of each system, DSC analysis was conducted. For statistic analysis, Kruskal-Wallis test and nonparametric Mann-Whitney U test post hoc were used for groups that did not show the normality and one-way analysis of variance and posh hoc Tukey test were used for other data.

In all three systems, the ultimate strength and toughness increased as the file size increased. The distortion angle of TN medium was significantly higher than that of TN small and prime, but there was no significant difference between others. WO and M3L tend to decrease in NCF as the size of the instrument increases, but in the case of TN, medium is significantly higher than small and prime. When comparing same size instruments of the different systems, WO and M3L showed no significant difference in both torsional resistance and cyclic fatigue resistance in the #20 size, and WO exhibited a higher distortion angle and toughness than the M3L in the #25 size. In the #35 size, the distortion angle and NCF of WO were significantly higher than those of M3L. On the other hand, M3L showed higher ultimate strength than WO. TN showed significantly lower ultimate strength and toughness than the other two systems and instruments of size #20 and #25 showed similar distortion angle as other systems, but instruments of size #35 were rather high. And #20, #25 size instruments showed a lower NCF than other systems, but #35 size was significantly higher than M3L and showed a similar rotation number to WO.

Within the limitations of the present study, as the size of file increases, the torsional resistance tends to increase. As the size of file increases, the cyclic fatigue resistance tends to decrease except for TN. Distortion angle might be more affected by the properties of Ni-Ti alloy than the size of Ni-Ti instrument. WO showed higher flexibility in a #35 size instrument than M3L, so it would be safer to use WO if #35 size instruments should be used in curved root canals. Since TN small and prime showed lower torsion and cyclic fatigue resistance than the other two systems, more care should be taken when using them.

Keywords : torsional resistance; cyclic fatigue resistance; nickel-titanium files; single-file system; scanning electron microscope; differential scanning calorimetry

Comparison of Torsional and Cyclic Fatigue Resistance of Various Nickel-titanium Single-file Systems

Gyeongha Son

Department of Dentistry
The Graduate School, Yonsei University
(Directed by Professor Sunil Kim)

I. Introduction

The file, a hand manipulation device for root canal treatment, was named 'K-type file (K-file)' and 'K-type reamer (K-reamer)' at Kerr manufacturing Co. in the early 1900s. It was produced in large quantities and the most used instrument in the 20th century. These instruments were used for canal cleaning and shaping by enlarging the root canal with insertion and withdrawal motions. Reamer, a type of file, enlarges the root canal through rotation. Depending on the cross-sectional design of the instrument or the number of spirals, it is classified whether it is the most suitable for filing or reaming. In general, a triangular shape with a small number of spirals is reaming, and a device having a triangular or square cross-section with a large number of spirals is used for filing.

Historically, the root canal instruments were made of carbon steel. After that, the quality of the instrument was significantly increased as it was manufactured using stainless-steel. Nevertheless, the stiffness of the stainless-steel instrument increases as the size of the instrument increases, and due to these characteristics, errors such as canal transportation appear when shaping curved root canals (Gambill et al., 1996; Gergi et al., 2010).

From the 1990s, rotary instruments made of Nickel-Titanium (Ni-Ti) alloy with superelasticity and shape memory characteristics were introduced in endodontists. Ni-Ti instruments have many advantages over conventional stainless-steel files, such as high flexibility, fewer canal deviation, high cutting efficiency, and shorter procedural time. (Schäfer et al., 2004) However, the Ni-Ti instruments were vulnerable to fracture and was recognized as one of the biggest drawbacks. In addition, because the Ni-Ti instruments are more expensive than conventional hand files, there is also a reuse problem. Reuse of instruments can also make them more vulnerable to fracture. Therefore, since the introduction of the Ni-Ti instruments, it has been developed to improve the cutting efficiency and centering ability, while reducing procedural errors and having high resistance to fracture.

In the mid-1990s, first generation Ni-Ti instruments were introduced to the market. Representatively, there are instruments such as LightSpeed endodontics (Lightspeed Technology, Inc., San Antonio, TX, USA), Profile (Dentsply Sirona, Ballaigues, Switzerland), Quantec (Kerr Corporation, Orange, CA, USA) and the most important feature of these is that they have passive cutting radial lands. There were studies that these instruments form smooth root canal walls and have fewer procedural errors, but they have the disadvantage of requiring numerous files (Hata et al., 2002; Yun and Kim, 2003).

To overcome these shortcomings, second generation instruments were introduced. This generation includes Protaper Universal (Dentsply Sirona), K3 (SybronEndo, Orange, CA, USA), and Mtwo (VDW, Munich, Germany), which have an active cutting edge to improve cutting efficiency. With fewer instruments than previous generation, root canal shaping is faster. At the same time, attempts were made to increase resistance to file separation. Several manufacturers have performed electropolishing to remove irregularities on the surfaces of instruments manufactured by traditional grinding methods. However, some degrees of canal transportation have been reported, and the risk of fracture still exists.

In 2007, manufacturers changed the properties of Ni-Ti alloys by applying heating and cooling technologies. The heat-treated alloy have a higher proportion of martensite than conventional instruments, which are more ductile, soft and flexible due to the characteristics of the martensite possessing the shape memory effect (Zhou et al., 2013). With the development of this heat treatment technology, M-wire, CM-wire, and R-phase were appeared, and third generation instruments with these alloys have higher flexibility and cyclic fatigue resistance than traditional instruments (Gao et al., 2012; Ha et al., 2013; Shim et al., 2017).

A feature of the fourth generation is the use of reciprocating motion. Reciprocation is defined as any repetitive back-and-forth or up-and-down motion, and is another development that can be used in the canal shaping and enlargement. A single-file technique was introduced along with reciprocating motion. WaveOne, which appeared on the market in 2011, advocated single-file system with reciprocating motion. It was rotated at an angle of 150 ° counterclockwise and 30 ° clockwise, which was designed not to exceed the elastic limit of the instrument. Others include Reciproc, self-adjusting file (SAF; ReDent-Nova, Raanana, Israel), etc.

In the fifth generation, the ability to shape a root canal was improved through offsetting the center of rotation. The offset designed file creates mechanical wave of motion along the active length of the instrument during rotation, thereby reducing engagement, taper lock and screw-in effects between the file and dentin, and improving cutting efficiency and removing the debris. This generation includes Protaper Next, Revo-S, One Shape, etc. (Goel et al., 2015; Kuzekanani, 2018)

As the manufacturing technology of Ni-Ti instruments has been developed, recent instruments can have increased flexibility and fracture resistance compared to traditional instruments. Therefore, while reducing procedural errors, the number of instruments required for cleansing and shaping during root canal treatment is reduced. As a result, several types of single file systems have been recently introduced to save time and make clinicians more convenient by simplifying instrumentation protocols and reduce mechanical stress (Bartols et al., 2016; Berutti et al., 2012; Bürklein et al., 2012). However, separation of Ni-Ti files is still unpredictable and it may lead to a poor prognosis (McGuigan et al., 2013).

Fracture modes of Ni-Ti files are commonly divided into two types, torsional and cyclic (flexural) fatigue fracture. Torsional fracture occurs when the tip of instrument tightly binds in the root canal, but motor that holds the shank of Ni-Ti file continues to rotate over the maximum strain which it can resist. Cyclic fatigue fracture occurs due to repeated compression and tensile stresses when an instrument rotates in a curved canal (McGuigan et al., 2013). To improve these shortcomings, manufacturers are making efforts to change the design of Ni-Ti file instruments or use new manufacturing processes, heat treatment, and surface treatment (Goo et al., 2017). Thermomechanical process changes the transformation temperatures of Ni-Ti alloy (Shen et al., 2013), which increases the flexibility and cyclic fatigue resistance (Goo et al., 2017; Plotino et al., 2014; Shen et al., 2013; Yahata et al., 2009).

In this study, Ni-Ti systems which are recently used and advocate single-file system, were selected; Waveone Gold (WO), M3-L Platinum (M3L), and Trunatomy (TN). Waveone Gold (Dentsply Sirona) has an off-centered parallelogram cross-section design. And it is used as reciprocating motion and special gold treatment are processed on the surface of the instrument, which helps the file to be more flexible and increase the cyclic fatigue resistance (Figure1.a) (De-Deus et al., 2010; Hieawy et al., 2015; Uygun et al., 2016). On the contrary M3-L platinum and Trunatomy are used as full-continuous rotational motion. M3-L platinum (United Dental Changzhou, Shanghai, China) is made from M-wire which is heat-treated Ni-Ti alloy, and according to the manufacturer, it has special geometry, patented flat-sided S-shaped cross section to reduce screw-in effect and to increase debris removal and efficient (Figure1.b).

Trunatomy (Dentsply Sirona), which provides slim shaping according to the recent trend of minimal invasive dentistry, was introduced (Figure1.c). Trunatomy also has an off-centered parallelogram cross-section design (Elnaghy et al., 2020). It is manufactured using a post-manufacturing thermal process and has smaller maximum flute diameter (0.8mm) than most of generic variable tapered Ni-Ti files (up to 1.2mm). It had been reported that the Trunatomy instruments preserve the structural dentin and tooth integrity due to instrument geometry, regressive tapers and the slim design, along with the heat treatment of the Ni-Ti alloy (Elnaghy et al., 2020; Pawar et al., 2014). These properties of Trunatomy are supposed to enhance the flexibility of the instrument (van der Vyver et al., 2019). Despite these advantages, however, the instruments are still vulnerable to fractures and clinicians are required to understand the fracture of the instruments.

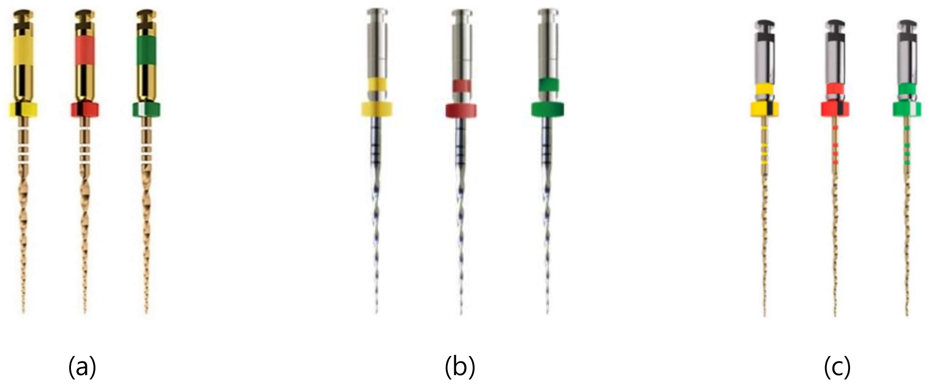

Figure 1. Ni-Ti instruments used in this study

(a) Waveone Gold, (b) M3-L platinum, (c) Trunatomy

So, the aim of this study is to investigate and compare the torsional and cyclic fatigue resistance among three different-sized Ni-Ti files of each single-file system and among same-sized Ni-Ti files of three different single-file systems, and to evaluate topographic of the fractured surface of instrument using scanning electron microscope (SEM) and identify the characteristics of each fracture mechanism. Also, to investigate the martensite/austenite transformation temperatures of the three systems using differential scanning calorimetry (DSC) analysis.

II. Materials and methods

Three brands of single-file systems (M3-L platinum, Waveone Gold and Trunatomy) and three different sizes of each system were selected. So, totally nine Ni-Ti groups were included; Waveone Gold Small (WOS; #20/.07, lot number:1565021), Waveone Gold Primary (WOP; #25/.07, lot number:1555104), Waveone Gold Medium (WOM; #35/.06, lot number:1567497), M3-L platinum L1(M3L1; #20/.07, lot number:M3LP21-L1), M3-L platinum L2(M3L2; #25/.065, lot number:M3LP21-L2), M3-L platinum L3(M3L3; #35/.06, lot number:M3LP321), Trunatomy Small (TNS; #20/.04, lot number:1593211), Trunatomy Prime (TNP; #26/.04, lot number:1578855) and Truntomy Medium (TNM; #36/.03, lot number:1593212). All files used in this study were 21mm long, and ten brand new instruments of each group were evaluated per test. All tests are conducted at room temperature.

Customized device (AendoS; DMJ System, Busan, Korea) was used for evaluation of cyclic fatigue and torsional resistance. Customized device consists of torque and weighing load cells, rotary motor, and connection part that can fix the shank of Ni-Ti instrument (Figure 2). Depending on the software settings, not only continuous rotary motion, but also reciprocating motion can be used and various actual root canal shaping processes can be mimicked.

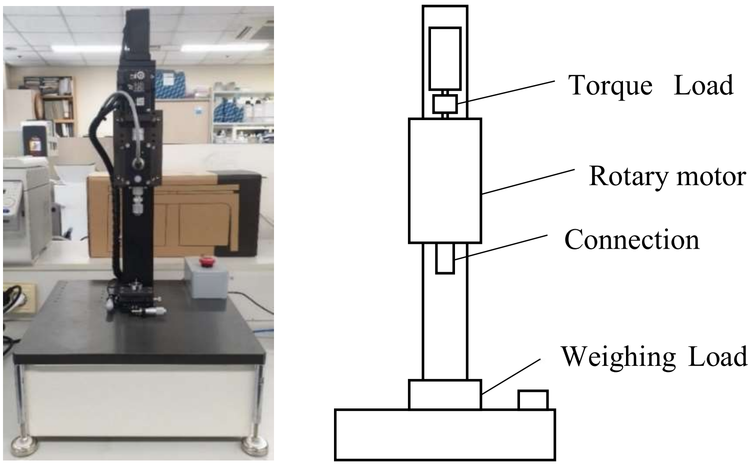

(a) (b)

Figure 2. (a) Customized device (AendoS) used in this study,
(b) Schematic diagram of the customized device

1. Torsional resistance

To evaluate the torsional resistance, 5mm apical part of the instrument was rigidly fixed between 2 polycarbonate blocks (Figure 3). Each instrument was rotated continuously at speed of 2 rpm until fracture occurred. Waveone Gold was driven counterclockwise because of the opposite direction of the spiral flutes. On the contrary, M3-L Platinum and Trunatomy were driven clockwise. The torsional load (Ncm) and distortion angle (°) were recorded during the test at the rate of 10 Hz. A stress(torsional load)-strain(distortion angle) curve was drawn using recorded data (figure 4). The ultimate load is maximum value of the measured torsional load, and distortion angle is angle of rotation of each file until fractured. To calculate the toughness (Ncm°), the area under the plot presenting distortion angle (X-axis) and torsional load (Y-axis) was computed by using Origin v6.0 Professional (Microcal Software Inc, Northampton, MA, USA).

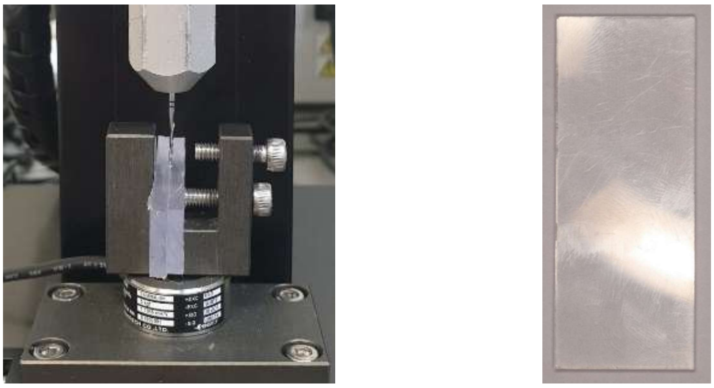

(a) (b)

Figure 3. Torsional resistance test. (a) 5mm apical part of Ni-Ti instrument was fixed between polycarbonate blocks. (b) Polycarbonate block used in the study

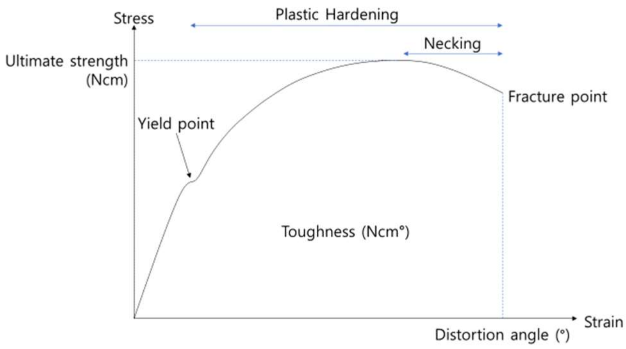

Figure 4. Typical stress-strain curve of a torsional resistance test. In the test, stress means torsional load, strain means distortion angle, and area under the curve means toughness.

2. Cyclic fatigue resistance

Cyclic fatigue resistance was evaluated in artificial canal block. This block was made of tempered steel with 5mm radius and 60° angle of curvature by the method described by Pruett (Pruett et al., 1997). And the point of maximum curvature was 5 mm from the tip of instrument.

There are two types of artificial canal blocks depending on the size of the file. When the width of the root canal becomes wider, the instrument follows less curvature than the planned trajectory (Plotino et al., 2009). Therefore, in order to make the instrument follow the planned curve as much as possible, blocks were produced by reflecting the taper of the instrument. Blocks used for experiments of #20 and 25 sized instruments have an apical of 0.6 mm, orifice of 1.0 mm, and blocks used for experiments of #35 sized instruments have apical of 0.6 mm and orifice of 1.5 mm width (Figure 5).

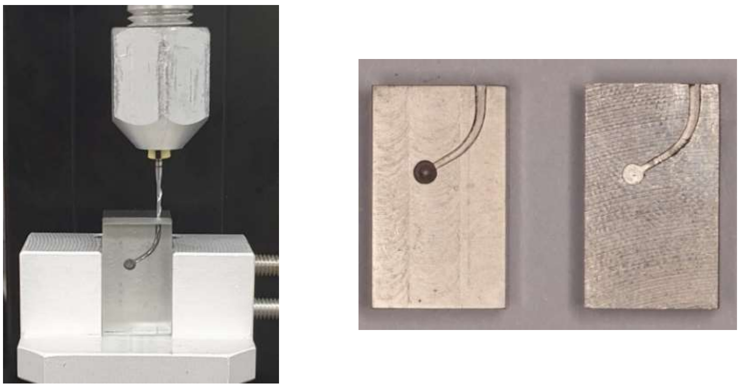

(a) (b)

Figure 5. Cyclic fatigue resistance test. (a) One side was covered with glass to observe the file optically. (b) Artificial canal blocks used in the study

The one side of metal block was covered with glass to observe the files optically. Synthetic oil (WD-40; WD-40 company, San Diego, CA, USA) was applied into the artificial canal before every test to reduce the friction between the instruments and the walls of metal block.

Each file system was evaluated according to the manufacturer's instructions. Waveone Gold was conducted using reciprocating rotation (350 rpm, 150° counterclockwise, 30° clockwise) and M3-L platinum, Trunatomy were conducted using continuous rotation (500 rpm). The experiment was conducted with 4 mm up-and-down pecking motion, and 8mm per second speed and 50 msec of dwell time. The time to fracture was measured visually and audibly, and recorded by using a digital chronometer. The number of cycles to fracture (NCF) for each instrument was calculated by multiplying the time (seconds) to failure by the number of rotations or cycles per second.

3. SEM Analysis

After torsional and cyclic fatigue resistance tests, fractured surfaces of instruments representing each group were evaluated using scanning electron microscope (SEM; Merlin, Carl ZEISS, Germany) to evaluate topographic of the fractured surface.

4. DSC analysis

To investigate the phase transformation temperatures, DSC analysis was used in which the difference between the heat energy supplied to the test specimen and inert control specimen heated at the same rate is measured accurately. WOM, M3L3, TNM of each single-file system were used for analysis. The samples were cut to a length of about 4 mm with a water-cooled, slow-speed diamond disc and about 15 mg of specimen was used. Each specimen was placed in an aluminum pan, and then placed in a DSC 200 F3 (NETZSCH, Selb, Deutschland) along with an empty aluminum reference pan. For each analysis, the specimen was first heated from room temperature to 100 °C at a rate of 10 °C/min and then cooled to -80 °C at a rate of -10°C/min. After that, it was heated to 100 °C again to obtain a heating/cooling DSC curve. To obtain the peak points and starting/finishing temperatures of the phase transformation, all data were analyzed with NETZSCH Proteus software. The staring and finishing temperatures were determined by the intersection of an extrapolated baseline and the maximum gradient line of the lambda-type DSC curve.

5. Statistic Analysis

The data were first analyzed by using the Shapiro-Wilk test for normality of distribution. Ultimate strength of WOP and toughness of TNS did not show the normality, Kruskal-Wallis test and nonparametric Mann-Whitney U test post hoc were used to analysis the data including ultimate strength of WOP and toughness of TNS. One-way analysis of variance and posh hoc Tukey test were used for other data. All statistical analyses were conducted at significant level of 95% using software (SPSS v25.0; IBM Corp, Somers, NY, USA).

III. Results

1. Comparisons according to file size within each single-file system

Table1 showed comparisons among files of different sizes within the same system. For WO, ultimate strength of WOM was significantly higher than those of the others, but the distortion angle did not differ among all three files. Toughness showed a significant increase as the size of the file increased. Conversely, NCF of WOS was significantly higher than those of the other two files (Figure 6).

For the M3L, the increase in file size resulted in a significant increase of the ultimate strength. And all three groups did not show significant differences on the distortion angle. Toughness of M3L3 was significantly higher than those of the others. Conversely, NCF showed significantly lower values only for M3L3 (Figure7).

In the case of TN, the ultimate strength and toughness increased significantly as the size of the file increased. For distortion angle and NCF, TNM showed significantly higher values than the other two files (Figure 8).

Table1. Comparisons of torsional and cyclic fatigue resistance among different-sized files of each single-file system

System	Instrument	Torsional resistance			Cyclic fatigue resistance
		Ultimate strength(Ncm)	Distortion angle(°)	Toughness(°Ncm)	NCF (Number of Cycles to Fracture)
Waveone Gold	WOS	2.19 ± 0.43^{B}	754.55 ± 80.56	1112.09 ± 186.82^{c}	2575 ± 359.19^{a}
	WOP	2.57 ± 0.15^{B}	732.34 ± 73.63	1395.28 ± 196.91^{b}	2080 ± 493.34^{b}
	WOM	3.23 ± 0.42^{A}	777.19 ± 99.27	1766.24 ± 333.39^{a}	1684 ± 217^{b}
M3-L Platinum	M3L1	2.06 ± 0.32^{c}	721.95 ± 179.62	1087.74 ± 433.16^{b}	2183 ± 656.06^{a}
	M3L2	2.65 ± 0.32^{b}	610.58 ± 60.53	1081.29 ± 107.45^{b}	2173 ± 489.50^{a}
	M3L3	3.98 ± 0.65^{a}	629.91 ± 94.77	1744.62 ± 380.08^{a}	1176 ± 151.35^{b}
Trunatomy	TNS	0.80 ± 0.05^{c}	749.62 ± 49.24^{b}	415.31 ± 52.56^{C}	1242 ± 206.49^{b}
	TNP	0.96 ± 0.07^{b}	729.76 ± 40.66^{b}	475.29 ± 49.63^{B}	1064 ± 99.07^{b}
	TNM	1.16 ± 0.06^{a}	952.48 ± 51.18^{a}	735.97 ± 81.19^{A}	1505 ± 278.92^{a}

Within each system, different superscript letters indicate statistical differences among instruments in vertical column ($P < .05$).

Groups with superscript capital letters were statistically analyzed with Kruskal-Wallis test and nonparametric Mann-Whitney U test post hoc.

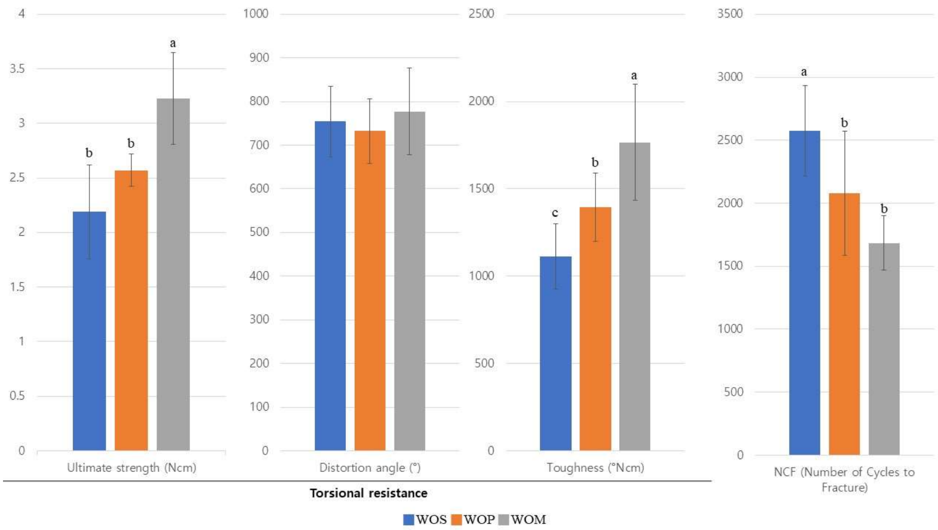

Figure 6. Comparisons of fracture resistance according to file size in Waveone Gold

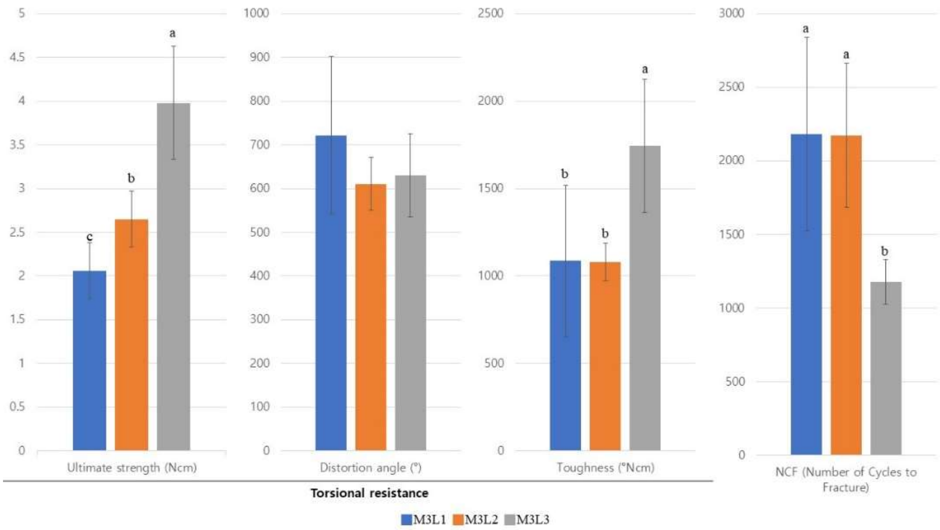

Figure 7. Comparisons of fracture resistance according to file size in M3-L Platinum

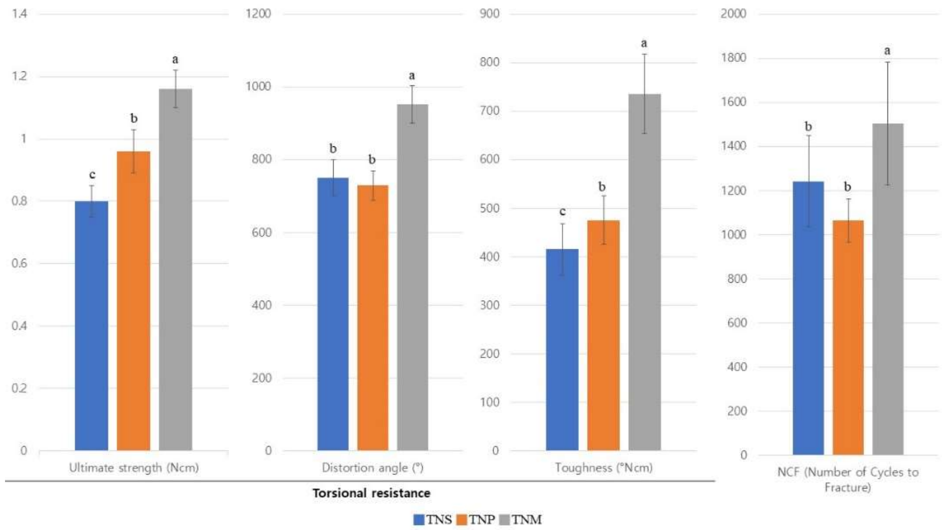

Figure 8. Comparisons of fracture resistance according to file size in Trunatomy

2. Comparisons among file systems according to file size

Table2 showed comparisons among instruments with the same tip size in different Ni-Ti file systems. In the comparisons among files in #20 tip size, the TNS in ultimate strength, toughness and NCF showed significantly lower values compared to the others, but the rest showed no significant difference (Figure 9).

In the comparisons among files of #25 tip size, there was no significant difference of ultimate strength between the WOP and M3L2, but TNP was the lowest. The distortion angle showed a significantly lower value for M3L2, and the other two files did not show significant difference. Toughness was the significantly highest in WOP, followed by M3L2 and TNP. For NCF, there was no difference between WOP and M3L2, and only TNP showed significantly lower value (Figure 10).

Comparisons among #35 tip sizes, ultimate strength of M3L3 was the highest and that of TNM was the lowest. And the distortion angle was significantly higher in the order of TNM, WOM, and M3L3. In the case of Toughness, there was no difference between WOM and M3L3, and only TNM showed significantly lower value. For the NCF, WOM and TNM did not show significant difference, and only M3L3 was significantly lower than others (Figure 11).

Table2. Comparisons of torsional and cyclic fatigue resistance among same-sized files of three different systems

Size of files	Instrument	Torsional resistance			Cyclic fatigue resistance
		Ultimate strength(Ncm)	Distortion angle(°)	Toughness(°Ncm)	NCF (Number of Cycles to Fracture)
#20	WOS	2.19 ± 0.43[a]	754.55 ± 80.56[a]	1112.09 ± 186.82[A]	2575 ± 359.19[a]
	M3L1	2.06 ± 0.32[a]	721.95 ± 179.62[a]	1087.74 ± 433.16[A]	2183 ± 656.06[a]
	TNS	0.80 ± 0.05[b]	749.62 ± 49.24[a]	415.31 ± 52.56[B]	1242 ± 206.49[b]
#25	WOP	2.57 ± 0.15[A]	732.34 ± 73.63[a]	1395.28 ± 196.91[a]	2080 ± 493.34[a]
	M3L2	2.65 ± 0.32[A]	610.58 ± 60.53[b]	1081.29 ± 107.45[b]	2173 ± 489.50[a]
	TNP	0.96 ± 0.07[B]	729.76 ± 40.66[a]	475.29 ± 49.63[c]	1064 ± 99.07[b]
#35	WOM	3.23 ± 0.42[b]	777.19 ± 99.27[b]	1766.24 ± 333.39[a]	1684 ± 217[a]
	M3L3	3.98 ± 0.65[a]	629.91 ± 94.77[c]	1744.62 ± 380.08[a]	1176 ± 151.35[b]
	TNM	1.16 ± 0.06[c]	952.48 ± 51.18[a]	735.97 ± 81.19[b]	1505 ± 278.92[a]

Within each same-sized group, different superscript letters indicate statistical differences among instruments in vertical column ($P < .05$).

Groups with superscript capital letters were statistically analyzed with Kruskal-Wallis test and nonparametric Mann-Whitney U test post hoc.

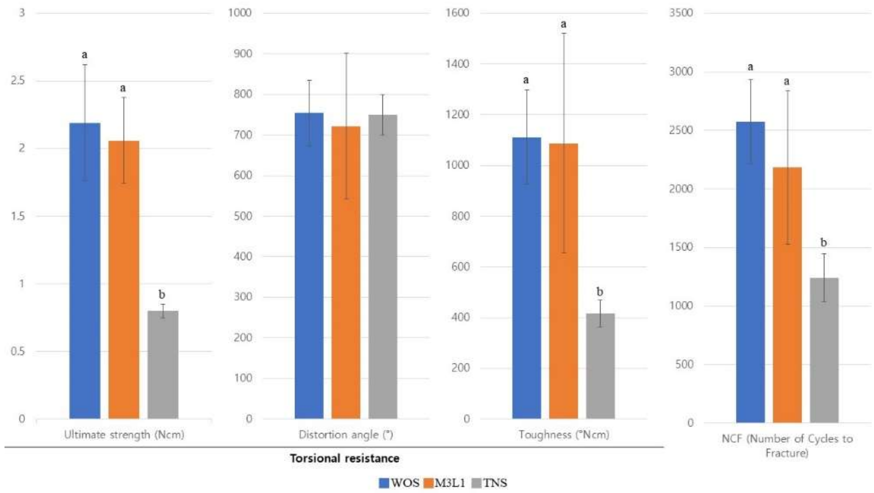

Figure 9. Comparisons among #20 size files of three single-file systems

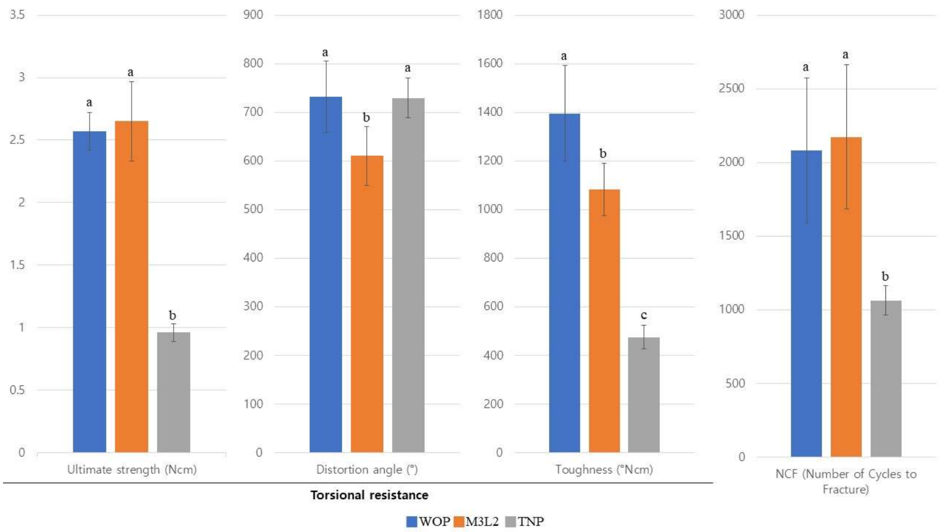

Figure 10. Comparisons among #25 size files of three single-file systems

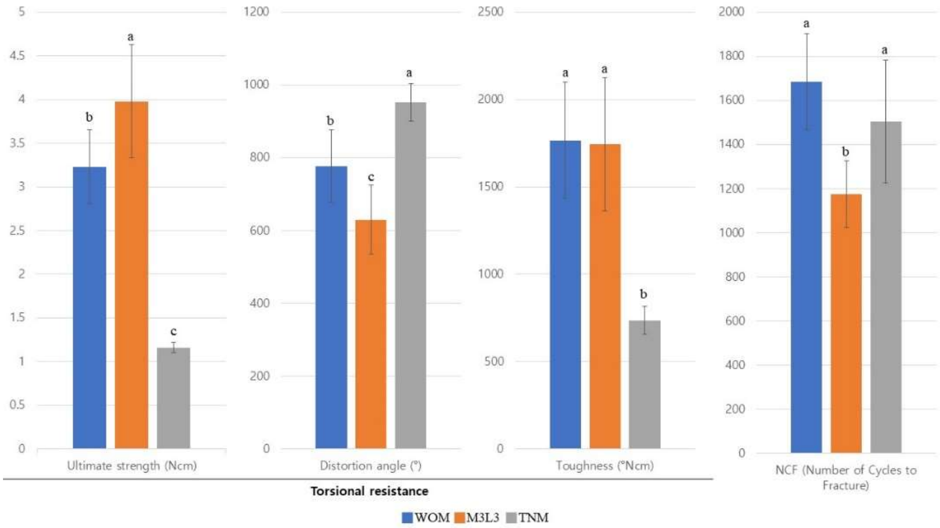

Figure 11. Comparisons among #35 size files of three single-file systems

3. SEM analysis of fractured surfaces of instruments

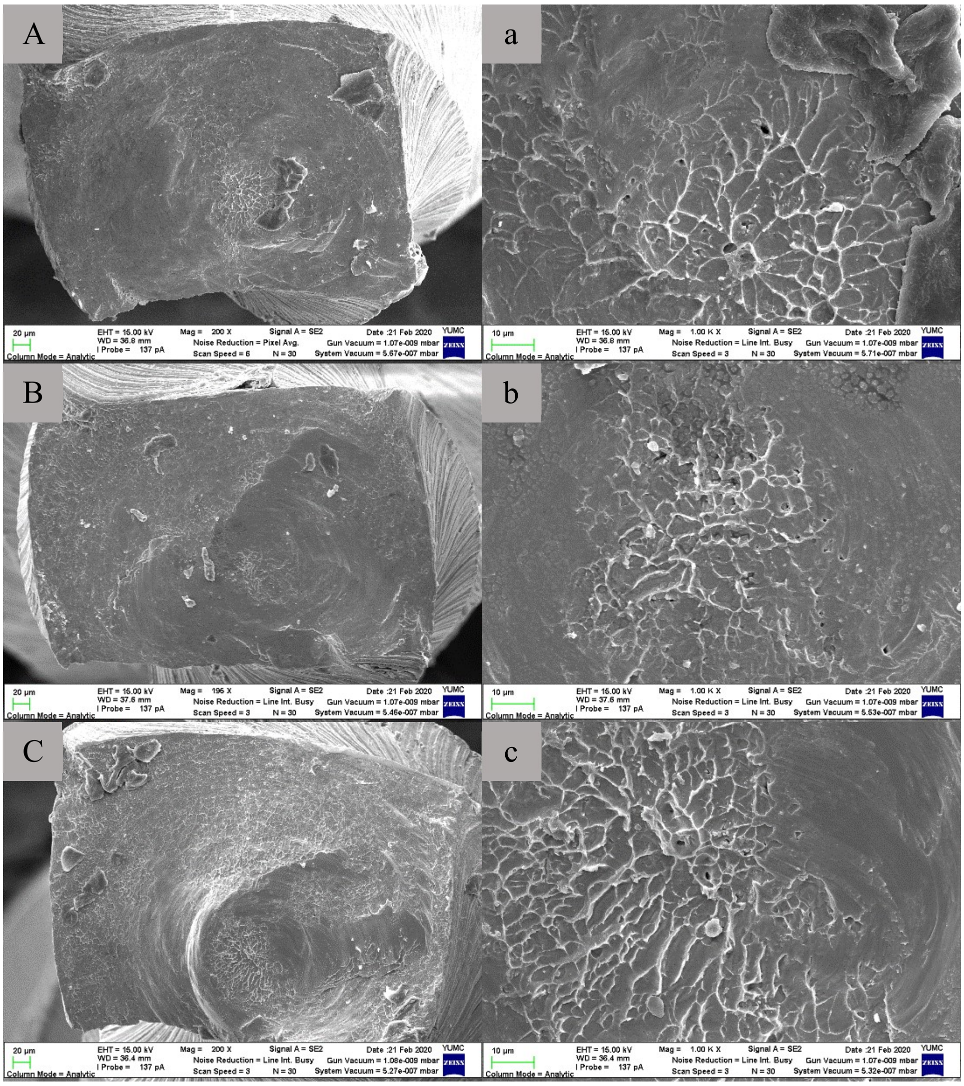

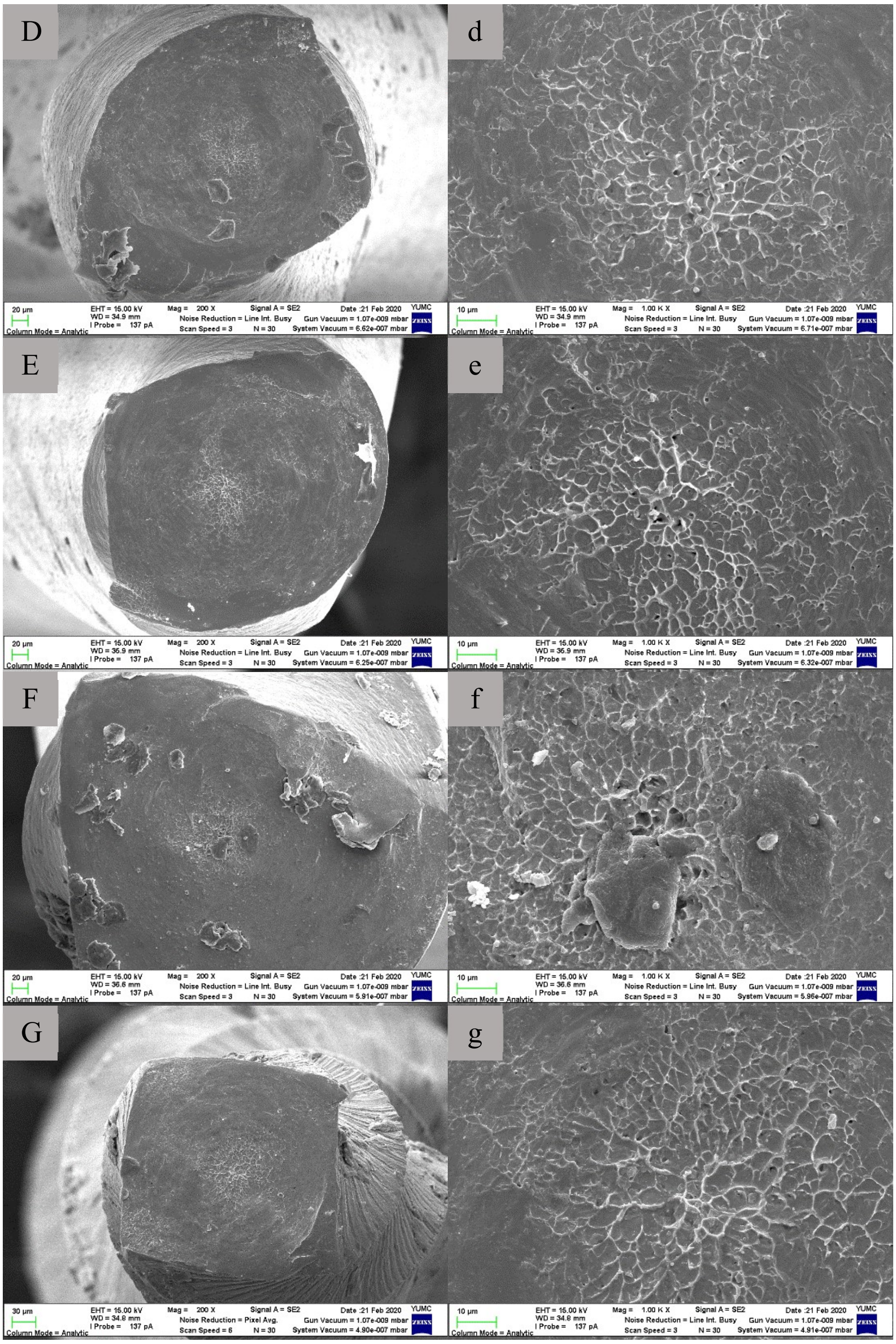
D
d
E
e
F
f
G
g

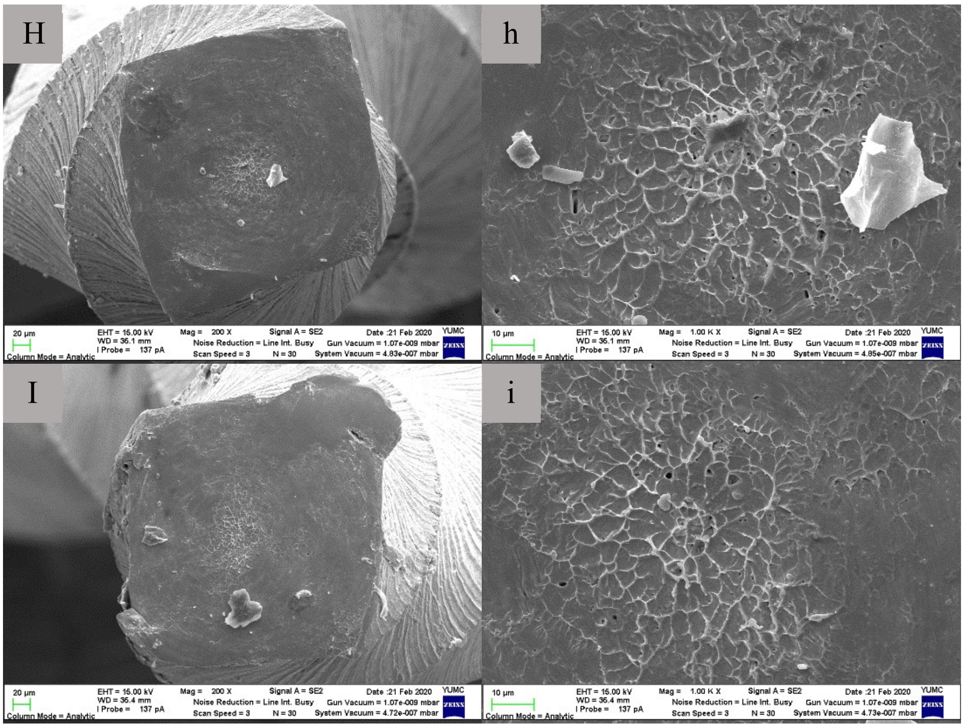

Figure 12. SEM images of the fractured surface of separated fragments in torsional test: (A, a) WOS, (B, b) WOP, (C, c) WOM, (D, d) M3L1, (E, e) M3L2, (F, f) M3L3, (G, g) TNS, (H, h) TNP, (I, i) TNM. All images show typical appearances of torsional fracture including circular abrasion marks at low magnification (A-I, x200) and skewed fibrous dimples near the center of rotation at higher magnification (a-i, x1000).

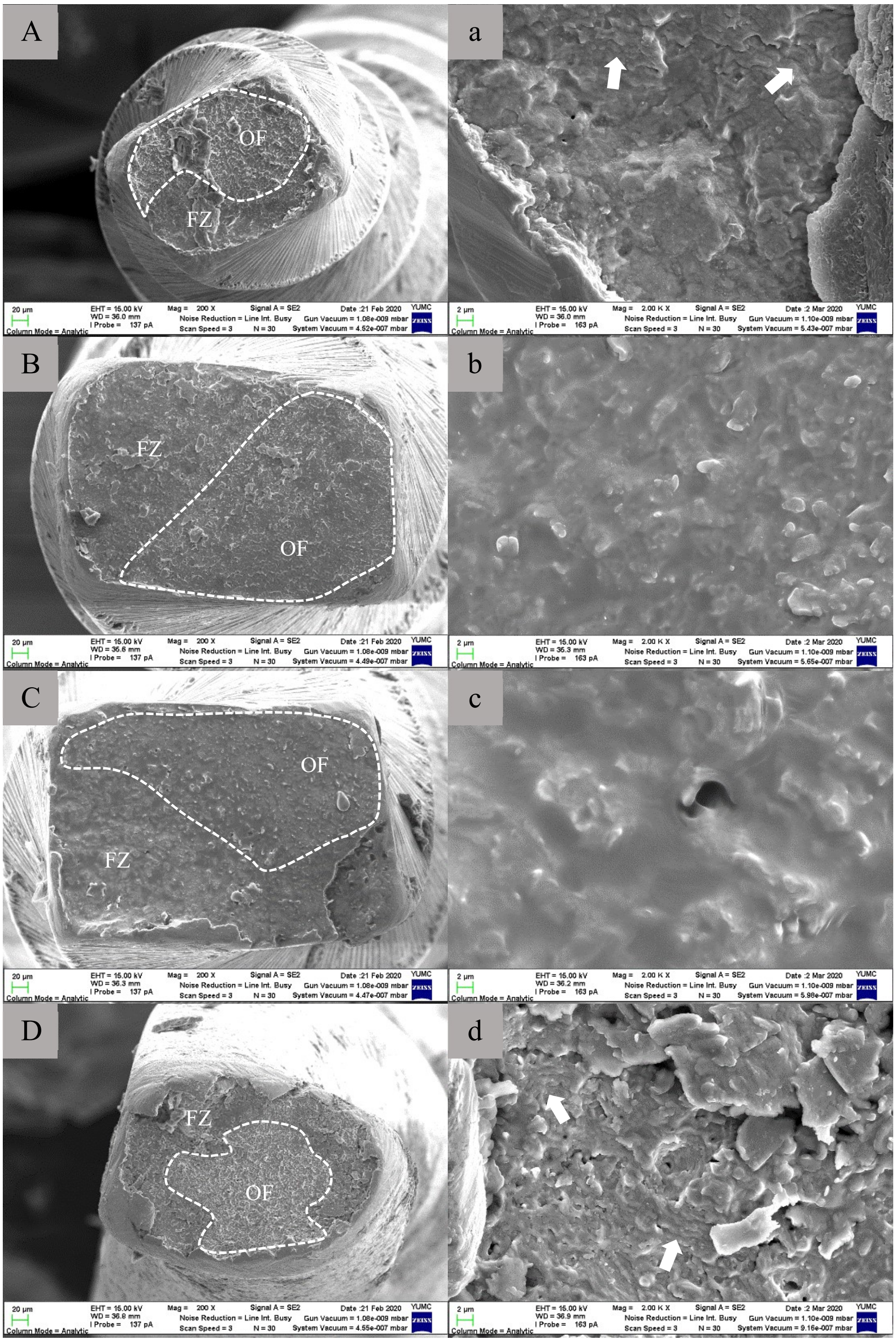
A
OF
FZ
a
B
FZ
OF
b
C
OF
FZ
c
D
FZ
OF
d

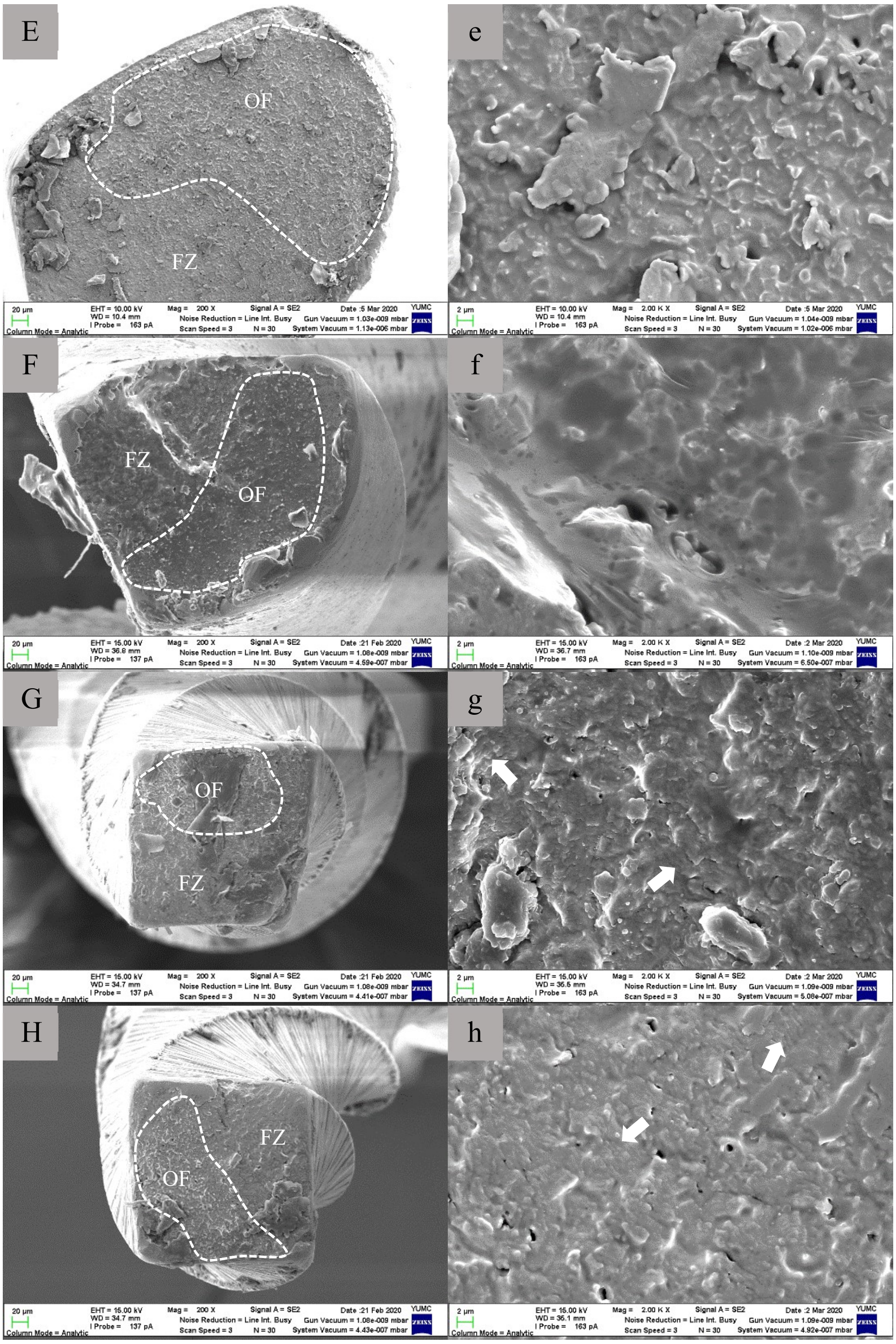
E
OF
FZ
e
F
FZ
OF
f
G
OF
FZ
g
H
FZ
OF
h

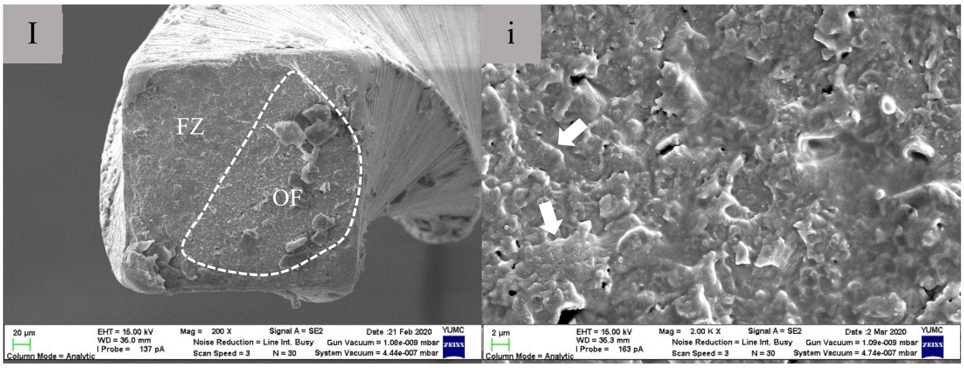

Figure 13. SEM images of the fractured surface of separated fragments in cyclic fatigue test: (A, a) WOS, (B, b) WOP, (C, c) WOM, (D, d) M3L1, (E, e) M3L2, (F, f) M3L3, (G, g) TNS, (H, h) TNP, (I, i). All image at low magnification (A-H, x200) show a mixed pattern of overload fast fracture zone (OF) and fatigue (slow fracture) zone (FZ). Dimple ruptures appear in overload fast fracture zone. At a high magnification (a-i, x2000), fatigue striations (white arrow) are observed in the fatigue zone.

4. DSC analysis

Two DSC curves are shown for each system, of which the left is the heating curve and the right is the cooling curve (Figure 14). Each curve has one or two peaks, which mean phase transformations. The endothermic peak in the heating curve represents austenitic transformation, the exothermic peak in the cooling curve represents martensitic transformation, and the additional peak represents R-phase transformation. So, the austenite start temperature (A_s) and austenite finish temperature (A_f) are located in the heating curve, and the martensite start temperature (M_s) and martensite finish temperature (M_f) are located in the cooling curve. R-phase start temperature (R_s) and R-phase finish temperature (R_f) can be obtained from the additional peak.

The DSC curves of WO and M3L have two consecutive endothermic peaks and one exothermic peak. In the heating curves, the peak on the left represents R-phase transformation, and the peak on the right represents austenitic transformation. And A_s of WO and M3L are higher than body temperature (Figure 14(a), (b)). The DSC curve of TN has two overlapped endothermic peaks (Figure 14(c)). These peaks indicate that the initial transformation from martensite to R-phase started at 16.6 °C, and immediately followed by transformation from R-phase to austenite at approximately 25 °C. At 30.8 °C, austenitic transformation was finished. Also, two separate exothermic peaks can be seen in cooling curve, the right one is R-phase transformation and the other is martensitic transformation. Each phase transformation start and finish temperature is provided in Table 3.

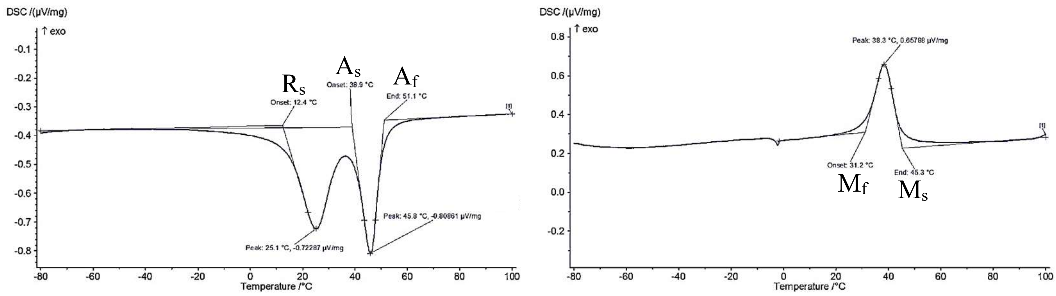

(a)

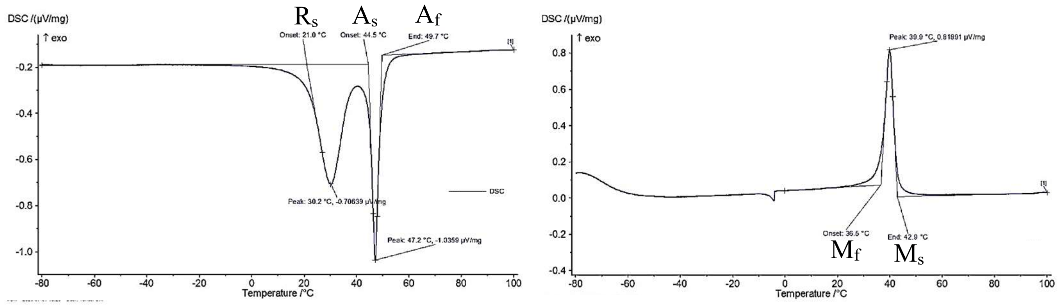

(b)

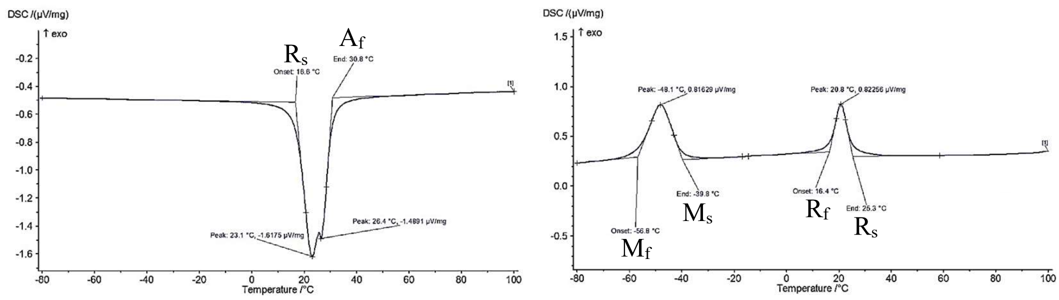

(c)

Figure 14. DSC curves of each single-file system. Each system has two curves, heating curve (left) and cooling curve (right). A_s and A_f are located in heating curve, and M_s and M_f are in cooling curve. R_s and R_f can be known from the curve with additional peak. (a) DSC curves of WO, (b) DSC curves of M3L, (c) DSC curves of TN

Table 3. Phase transformation temperatures of each single-file system from DSC analysis

Cooling				
System	M_s (°C)	M_f (°C)	R_s (°C)	R_f (°C)
WO	45.3	31.2	-	-
M3L	42.9	36.5	-	-
TN	-39.8	-56.8	25.3	16.4

Heating				
System	R_s (°C)	R_f (°C)	A_s (°C)	A_f (°C)
WO	12.4	-	38.9	51.1
M3L	21	-	44.5	49.7
TN	16.6	-	-	30.8

IV. Discussion

Ni-Ti rotary instruments are widely used in nonsurgical endodontic treatment due to many advantages, including the convenience of the operator, but there is still a risk of instrument fractures. File separation itself does not cause endodontic failure (Spili et al., 2005), but it can block canal, negatively affecting the success rate of root canal treatment. One study reported that 70% of the fractures are caused by the cyclic fatigue and only 30% of the others are caused by the torsional stress (Parashos et al., 2004). Therefore, many manufacturers make efforts to increase the fatigue resistance of the instruments. One way of doing that is to modify the properties of Ni-Ti alloy with the thermomechanical process and the Ni-Ti files used in this study were made from heat-treated Ni-Ti alloy.

The properties of Ni-Ti alloys could be changed by applying heating and cooling technologies. Ni-Ti alloy has three microstructural phases (austenite, martensite, R-phase), and the properties of the alloy vary depending on their relative proportions (Shen et al., 2013). When the martensite is heated, it changes to austenite. The temperature at this starting point is called austenite start temperature, and the temperature at which all martensite turns into austenite is called austenite finish temperature (Thompson, 2000; Zupanc et al., 2018). Conventional Ni-Ti instruments have an austenite finish temperature similar to or lower than the root temperature, so that most of the instruments in clinical use consist of austenite. However, the heat-treated instruments have higher the austenite finish temperature, thereby increasing the proportion of martensite in clinical use (Shen et al., 2013). In this way, M-wire, CM-wire, and R-phase appeared, and the instruments manufactured using them were softer and ductile, and increased the cyclic fatigue resistance to lower the risk of fracture (Gao et al., 2012; Ha et al., 2013; Shim et al., 2017). DSC analysis is generally used to study the properties of Ni-Ti alloy, which is one of the major influential factors of mechanical and metallurgical characteristics of Ni-Ti instruments. By this analysis, phase transformation temperatures of the alloy could be known, and this information helps a lot in understanding the characteristics of Ni-Ti instruments (Brantley et al., 2002).

Factors such as the operator's handling, usage, and anatomical shape of the tooth, as well as the cross-section design of the instrument, diameter, number of spirals, and Ni-Ti alloy type can affect the fracture of the instrument (Cheung et al., 2007; Lopes et al., 2013). Therefore, if a new instrument is released, it will be important to understand its characteristics for safety use.

In the torsional resistance test, a high ultimate strength means that the instrument can withstand higher torque forces, which can be used to enlarge the root canal using a stronger torque force. In Table 1, it can be seen that in all three groups, the ultimate strength increases as the file size increases. According to Yum et al., the cross-section dimension has a major influence on yield strength and ultimate strength. That is, as the cross-section dimension is larger, the ultimate strength value increases. If instruments have the same Ni-

Ti alloy and cross-section design and only increase the dimension, the ultimate strength will increase like results of this study, which is consistent with the results of previous studies (Yum et al., 2011). In Table 2, the torsional resistance of WOS and M3L1 does not show a significant difference, and the ultimate strengths of WOP and M3L2 also do not show a significant difference. In #35 size files, M3L3 shows greater ultimate strength than WOM, but has a lower distortion angle. According to previous studies, CM-wire or R-phase instruments have lower modulus of elasticity and higher flexibility than M-wire or traditional instruments, and this difference results in lower ultimate strength but higher distortion angle (Shim et al., 2017; Silva et al., 2019). Also, gold heat-treated instruments have higher flexibility and fatigue resistance than conventional Ni-Ti and M-wire Ni-Ti (Hieawy et al., 2015; Keskin et al., 2017; Topçuoğlu et al., 2017). Therefore, the gold heat-treated instrument, WO, shows a lower or similar ultimate strength value than the M3L (M-wire). In the case of TN, it showed the lowest ultimate strength because it has lower cross-section dimensions than the other two files (Yum et al., 2011).

The distortional angle in torsional resistance refers to the instrument's ductility, which means the instrument's ability to be plastically deformed under stress without fracture. The higher the flexibility of the instrument, the higher the value of the distortion angle, which makes the instrument safer to use (increase the safety zone) (Shim et al., 2017; Silva et al., 2019). If the cutting spiral is deformed during clinical use, it indicates that the plastic deformation occurred before the instrument was fractured, informing the clinician of the risk of fracture of the instrument. In the case of WO and M3L, the distortion angle has no significant difference regardless of the size of the file. According to previous studies, the lower the yield strength of the instrument, the more flexible and ductile it is, and yield strength is more affected by the properties of the Ni-Ti alloy than taper (Ha et al., 2013; Yum et al., 2011). In summary, the distortion angle is also more likely to be influenced by the properties of the Ni-Ti alloy than the taper of the instrument, and considering the results of this study, the properties of the Ni-Ti alloy are more important than the size of the file. So, the more flexible WO (Gold heat-treated) has a higher distortion angle value than M3L (M-wire). TNS and TNP do not show a significant difference, but TNM shows an increased distortion angle. TN, unlike the other two instruments, has a small taper of .03 or .04, and a small dimension at 5mm from the tip. It is speculated that excessively small dimension of TNS and TNP reduces instrument’s ductility. In addition, TN showed similar or higher distortion angle than those of other systems, even though the austenitic transformation temperature of TN is lower. As a result, the distortion angle might be more affected by the properties of Ni-Ti alloy than the size of the file, but it is presumed that other factors such as the design of instrument also seem to have impacts. Further research is needed to evaluate effects of other factors for distortion angle.

Toughness is calculated as the total area of the stress-strain curve, which is the total amount of energy absorbed before the instrument fractures (Yum et al., 2011). While this indicator cannot be said to represent the torsional resistance of the instrument, it may help to understand the instrument's fracture along with ultimate strength and distortion angle. In Table 1, in all three groups, as file size increased, toughness tended to increase. This is because the cross-sectional area of the instrument becomes wider and the ultimate strength increases, but the distortion angle does not differ significantly. In Table 2, TN shows a lower toughness value compared to other system files. This is considered to be because the distortion angle is similar, but the cross-sectional dimension is smaller and shows a much lower ultimate strength. Although the ultimate strength of WO is lower than that of M3L, the distortion angle tends to be high, and even when toughness is calculated, there is no significant difference except for the #25 size instrument.

Cyclic fatigue fracture, unlike torsional fracture, does not show plastic deformation of the instrument, and is more difficult to predict because fatigue accumulates and breaks suddenly. Therefore, it is important to use instruments with high cyclic fatigue resistance in the root canal with severe curvature to reduce the possibility of fracture. In general, the NCF decreases as the instrument diameter of the maximum curved region increases. This is because the farther from the center of the instrument, the higher the compression and tensile stress (Plotino et al., 2006). WO and M3L tend to decrease in NCF as the size of the instrument increases, which is consistent with previous study. In the TN group, NCF of TNP is lower than that of TNS, but there is no significant difference. On the contrary, TNM shows rather higher NCF. This is supposed to be due to the difference in experimental methods. WOM and M3L3 have a large diameter, so they were tested in a block with a wide width. TNM also has the #35 tip size, so it was tested in the same block. It may rotate in a path with a larger radius and a reduced angle than the planned curve due to the nature of spring back into its original straight shape (Plotino et al., 2009), which may lead a higher

NCF value. In Table 2, there was no significant difference between WOS and M3L1, WOP and M3L2, but WOM showed a significantly higher value than M3L3. This is because the gold heat-treated instrument is more flexible than the M-wire (Zupanc et al., 2018), and WO was rotated in reciprocating motion, and M3L was in rotational motion. According to previous study, cyclic fatigue life increased when using the instrument as a reciprocating motion (De-Deus et al., 2010). TNS and TNP showed significantly lower NCF compared to the same-sized Ni-Ti instruments of other systems. This is because TN has lower austenitic transformation temperature compared to other systems. At room temperature, WO and M3L are composed of stable martensite and R-phase, while TN is composed of austenite in some portion of the alloy, which results in reduced flexibility and lower NCF (Shim et al., 2017). Since body temperature is higher than A_f of TN, the flexibility of TN would decrease further when used in clinical condition.

Among the instruments used in the experiment, the fracture surface of the instrument having the most similar value to the mean of each group was observed through SEM. In order to classify the mode of fracture, it is more accurate to observe the features of the fracture surface at high magnification than the side of the instrument at low magnification (Cheung et al., 2005). In Figure 12, a typical appearances of torsional fracture was observed. Circular abrasion is observed at low magnification and at high magnification, fatigue striations are absent and skewed fibrous dimples are observed near the center of rotation (Shen et al., 2009). In the case of fatigue fracture, microcracks are first formed on the surface flaws or irregularities where stress is concentrated. Therefore, the machining grooves remaining on the instruments after the manufacturing process can be the origin for cracks. After the microcrack is formed, it propagates gradually as the compression and tension stress is repeated (Cheung et al., 2005). As the microcracks gradually progress (fatigue zone), fatigue striations are typically observed in this area. If the remaining intact material cannot withstand the stress, the instrument is fractured (overload fast fracture zone), and dimple ruptures are typically observed in this region (Cheung and Darvell, 2007; Goo et al., 2017) (Figure 13).

V. Conclusions

Within the limitations of the present study, as the size of file increases, the torsional resistance tends to increase. As the size of file increases, the cyclic fatigue resistance tends to decrease except for TN. Distortion angle might be more affected by the properties of Ni-Ti alloy than the size of Ni-Ti instrument. WO showed higher flexibility in a #35 size instrument than M3L, so it would be safer to use WO if #35 size instruments should be used in curved root canals. Since TNS and TNP showed lower torsion and cyclic fatigue resistance than the other two systems, more care should be taken when using them.

VI. Acknowledgements

Thanks to Professor Jaesung Gwon and Jaekyung Lee of Department & Research Institute of Dental Biomaterials and Bioengineering, Yonsei University College of Dentistry for conducting DSC analysis.

References

Bartols A, Laux G, Walther W (2016). Multiple-file vs. single-file endodontics in dental practice: a study in routine care. PeerJ 4: e2765.

Berutti E, Chiandussi G, Paolino DS, Scotti N, Cantatore G, Castellucci A, et al. (2012). Canal shaping with WaveOne Primary reciprocating files and ProTaper system: a comparative study. Journal of endodontics 38(4): 505-509.

Brantley W, Svec T, Iijima M, Powers J, Grentzer T (2002). Differential scanning calorimetric studies of nickel titanium rotary endodontic instruments. Journal of endodontics 28(8): 567-572.

Bürklein S, Hinschitza K, Dammaschke T, Schäfer E (2012). Shaping ability and cleaning effectiveness of two single-file systems in severely curved root canals of extracted teeth: Reciproc and WaveOne versus Mtwo and ProTaper. International endodontic journal 45(5): 449-461.

Cheung G, Darvell B (2007). Fatigue testing of a NiTi rotary instrument. Part 2: fractographic analysis. International endodontic journal 40(8): 619-625.

Cheung G, Peng B, Bian Z, Shen Y, Darvell B (2005). Defects in ProTaper S1 instruments after clinical use: fractographic examination. International Endodontic Journal 38(11): 802-809.

Cheung GS, Shen Y, Darvell BW (2007). Effect of environment on low-cycle fatigue of a nickel–titanium instrument. Journal of endodontics 33(12): 1433-1437.

De-Deus G, Moreira E, Lopes H, Elias C (2010). Extended cyclic fatigue life of F2 ProTaper instruments used in reciprocating movement. International endodontic journal 43(12): 1063-1068.

Elnaghy AM, Elsaka SE, Mandorah AO (2020). In vitro comparison of cyclic fatigue resistance of TruNatomy in single and double curvature canals compared with different nickel-titanium rotary instruments. BMC Oral Health 20(1): 38.

Gambill JM, Alder M, Carlos E (1996). Comparison of nickel-titanium and stainless steel hand-file instrumentation using computed tomography. Journal of Endodontics 22(7): 369-375.

Gao Y, Gutmann JL, Wilkinson K, Maxwell R, Ammon D (2012). Evaluation of the impact of raw materials on the fatigue and mechanical properties of ProFile Vortex rotary instruments. Journal of endodontics 38(3): 398-401.

Gergi R, Rjeily JA, Sader J, Naaman A (2010). Comparison of canal transportation and centering ability of twisted files, Pathfile-ProTaper system, and stainless steel hand K-files by using computed tomography. Journal of Endodontics 36(5): 904-907.

Goel A, Rastogi R, Rajkumar B, Choudary T, Boruah L, Gupta V (2015). An overview of modern endodontic NiTi systems. Med Sci 4: 2277-8179.

Goo H-J, Kwak SW, Ha J-H, Pedullà E, Kim H-C (2017). Mechanical properties of various heat-treated nickel-titanium rotary instruments. Journal of endodontics 43(11): 1872-1877.

Ha J-H, Kim SK, Cohenca N, Kim H-C (2013). Effect of R-phase heat treatment on torsional resistance and cyclic fatigue fracture. Journal of endodontics 39(3): 389-393.

Hata G-i, Uemura M, Kato AS, Imura N, Novo NF, Toda T (2002). A comparison of shaping ability using ProFile, GT file, and Flex-R endodontic instruments in simulated canals. Journal of endodontics 28(4): 316-321.

Hieawy A, Haapasalo M, Zhou H, Wang Z-j, Shen Y (2015). Phase transformation behavior and resistance to bending and cyclic fatigue of ProTaper Gold and ProTaper Universal instruments. Journal of endodontics 41(7): 1134-1138.

Keskin C, Inan U, Demiral M, Keleş A (2017). Cyclic fatigue resistance of Reciproc Blue, Reciproc, and WaveOne Gold reciprocating instruments. Journal of endodontics 43(8): 1360-1363.

Kuzekanani M (2018). Nickel–Titanium rotary instruments: Development of the single-file systems. Journal of International Society of Preventive & Community Dentistry 8(5): 386.

Lopes HP, Gambarra-Soares T, Elias CN, Siqueira Jr JF, Inojosa IF, Lopes WS, et al. (2013). Comparison of the mechanical properties of rotary instruments made of conventional nickel-titanium wire, M-wire, or nickel-titanium alloy in R-phase. Journal of endodontics 39(4): 516-520.

McGuigan M, Louca C, Duncan H (2013). Endodontic instrument fracture: causes and prevention. British dental journal 214(7): 341.

Parashos P, Gordon I, Messer HH (2004). Factors influencing defects of rotary nickel-titanium endodontic instruments after clinical use. Journal of endodontics 30(10): 722-725.

Pawar AM, Pawar MG, Kokate SR (2014). Meant to make a difference, the clinical experience of minimally invasive endodontics with the self-adjusting file system in India. Indian Journal of Dental Research 25(4): 509.

Plotino G, Grande NM, Cordaro M, Testarelli L, Gambarini G (2009). A review of cyclic fatigue testing of nickel-titanium rotary instruments. Journal of endodontics 35(11): 1469-1476.

Plotino G, Grande NM, Cotti E, Testarelli L, Gambarini G (2014). Blue treatment enhances cyclic fatigue resistance of vortex nickel-titanium rotary files. Journal of endodontics 40(9): 1451-1453.

Plotino G, Grande NM, Sorci E, Malagnino V, Somma F (2006). A comparison of cyclic fatigue between used and new Mtwo Ni–Ti rotary instruments. International Endodontic Journal 39(9): 716-723.

Pruett JP, Clement DJ, Carnes Jr DL (1997). Cyclic fatigue testing of nickel-titanium endodontic instruments. Journal of endodontics 23(2): 77-85.

Schäfer E, Schulz-Bongert U, Tulus G (2004). Comparison of hand stainless steel and nickel titanium rotary instrumentation: a clinical study. Journal of endodontics 30(6): 432-435.

Shen Y, Cheung GS-p, Peng B, Haapasalo M (2009). Defects in nickel-titanium instruments after clinical use. Part 2: fractographic analysis of fractured surface in a cohort study. Journal of endodontics 35(1): 133-136.

Shen Y, Zhou H-m, Zheng Y-f, Peng B, Haapasalo M (2013). Current challenges and concepts of the thermomechanical treatment of nickel-titanium instruments. Journal of endodontics 39(2): 163-172.

Shim K-S, Oh S, Kum K, Kim Y-C, Jee K-K, Chang SW (2017). Mechanical and metallurgical properties of various nickel-titanium rotary instruments. BioMed research international 2017.

Silva E, Giraldes J, de Lima C, Vieira V, Elias C, Antunes H (2019). Influence of heat treatment on torsional resistance and surface roughness of nickel-titanium instruments. International endodontic journal 52(11): 1645-1651.

Spili P, Parashos P, Messer HH (2005). The impact of instrument fracture on outcome of endodontic treatment. Journal of endodontics 31(12): 845-850.

Thompson S (2000). An overview of nickel–titanium alloys used in dentistry. International endodontic journal 33(4): 297-310.

Topçuoğlu H, Düzgün S, Aktı A, Topçuoğlu G (2017). Laboratory comparison of cyclic fatigue resistance of WaveOne Gold, Reciproc and WaveOne files in canals with a double curvature. International endodontic journal 50(7): 713-717.

Uygun A, Kol E, Topcu M, Seckin F, Ersoy I, Tanriver M (2016). Variations in cyclic fatigue resistance among ProTaper Gold, ProTaper Next and ProTaper Universal instruments at different levels. International endodontic journal 49(5): 494-499.

van der Vyver PJ, Vorster M, Peters OA (2019). Minimally invasive endodontics using a new single-file rotary system. Int Dent–African ed 9(4): 6-20.

Yahata Y, Yoneyama T, Hayashi Y, Ebihara A, Doi H, Hanawa T, et al. (2009). Effect of heat treatment on transformation temperatures and bending properties of nickel–titanium endodontic instruments. International endodontic journal 42(7): 621-626.

Yum J, Cheung GS-P, Park J-K, Hur B, Kim H-C (2011). Torsional strength and toughness of nickel-titanium rotary files. Journal of endodontics 37(3): 382-386.

Yun H-h, Kim SK (2003). A comparison of the shaping abilities of 4 nickel-titanium rotary instruments in simulated root canals. Oral Surgery, Oral Medicine, Oral Pathology, Oral Radiology, and Endodontology 95(2): 228-233.

Zhou H, Peng B, Zheng YF (2013). An overview of the mechanical properties of nickel–

titanium endodontic instruments. Endodontic topics 29(1): 42-54.

Zupanc J, Vahdat-Pajouh N, Schäfer E (2018). New thermomechanically treated NiTi alloys–a review. International endodontic journal 51(10): 1088-1103.

Abstract (In Korean)

다양한 니켈-타이타늄 Single-file 시스템의 비틀림 저항성과 피로 파절 저항성의 비교

손 경 하

연세대학교 대학원

치의학과

(지도교수 김 선 일)

본 연구의 목적은 같은 니켈-타이타늄 single-file 시스템 내에서 서로 다른 사이즈를 가지는 세가지 파일 사이의 비틀림 저항성과 피로 파절 저항성을 비교하고, 같은 사이즈를 가지는 서로 다른 세가지 니켈-타이타늄 single-file 시스템 사이의 비틀림 저항성과 피로 파절 저항성을 비교하는 것이다. 그리고 기구의 파절된 면을 주사전자현미경을 통해 관찰해 파절 메커니즘에 따

른 특징을 확인하고, 또한 시차주사 열량측정법을 통해 세 시스템의 상 변이 온도를 조사하는 것이다.

연구에는 세 종류의 single-file 시스템(Waveone Gold[WO]; Dentsply Sirona, Ballaigues, Switzerland, M3-L platinum[M3L]; United Dental Changzhou, Shanghai, China and Trunatomy[TN]; Dentsply Sirona)이 선택되었으며, 각각의 시스템에서 세가지 사이즈(#20, #25, #35)의 파일을 사용하였다. 모든 실험에는 각 군당 10개씩 새 기구를 사용하였으며, 비틀림 저항을 평가하기위해 2개의 폴리카보네이트 블록 사이에 파일의 끝 5 mm를 고정시키고, 2 rpm의 속도로 파일이 파절될 때까지 회전시켰으며, 피로 파절 저항성의 측정을 위해 각각의 파일을 인공 근관 블럭 내에서 회전시켜 파절 될 때까지의 회전수를 측정하였다. 파절 실험 후, 각각의 그룹을 대표하는 파일의 파절면을 주사전자현미경을 통해 관찰하였다. 그리고 각 시스템의 상 변이 온도를 측정하기 위해 시차주사 열량측정법을 시행하였다. 정규성을 따르지 않는 그룹은 Kruskal-Wallis test와 nonparametric Mann-Whitney U test post hoc을 이용하였으며, 나머지 그룹은 one-way analysis of variance와 posh hoc Tukey test를 이용하여 통계 분석을 시행하였다.

모든 그룹에서 파일의 사이즈가 커질수록, 최고 비틀림 응력값과 인성은 증가하였다. TN medium의 비틀림 변형량은 TN small과 prime에 비해 유의

미하게 높았지만, WO과 M3L에서는 차이가 없었다. WO과 M3L은 파일의 사이즈가 커질수록 파절 될 때까지의 회전수는 감소하였으나, TN medium은 TN small과 prime보다 유의미하게 높았다. 서로 다른 시스템의 같은 사이즈 파일을 비교해보면, #20 사이즈에서 WO과 M3L은 비틀림 저항성과 피로 파절 저항성 모두 유의미한 차이를 보이지 않았다. #25 사이즈에서는 WO가 M3L에 비해 높은 비틀림 변형량을 보였다. #35 사이즈에서는 WO의 비틀림 변형량과 파절 될 때까지의 변형량이 M3L에 비해 유의미하게 높았으나, 반대로 M3L이 더 높은 최고 비틀림 응력값을 보였다. TN은 다른 두 시스템에 비해 낮은 최고 비틀림 응력값과 인성을 보였다. #20, #25 사이즈의 TN은 다른 시스템의 기구와 비슷한 비틀림 변형량을 보이고, 파절 될 때까지의 회전수는 적었지만, #35 사이즈의 기구는 오히려 높은 비틀림 변형량을 가졌으며, 회전 수 또한 M3L보다 높고 WO과 비슷하게 나타났다..

결론적으로, 파일의 사이즈가 커질수록 비틀림 저항성은 증가하는 경향을 보인다. TN을 제외하고는 파일의 사이즈가 커질수록 피로 파절 저항성은 감소하는 경향을 보인다. 비틀림 변형량은 기구의 크기보다는 니켈-타이타늄 합금의 특성에 더 많은 영향을 받는 것으로 보인다. #35 사이즈의 기구에서 WO이 M3L보다 더 높은 유연성을 보여주었기 때문에, 만곡된 근관에서 사용한다면 WO을 사용하는 것이 더 안전할 것이다. TN small과 prime은 다른 시스템에 비해 낮은 비틀림 저항성 및 피로 파절 저항성을 보이기 때문에, 사용

할 때 더 많은 주의가 필요할 것이다.

핵심 되는 말 : 비틀림 저항성; 피로 파절 저항성; 니켈-타이타늄 파일; single-file 시스템; 주사전자현미경; 시차주사 열량측정법